의학석사 학위논문

The Study of Neuroinflammation and Blood-Brain Barrier Disruption in Early Stage Alzheimer's Disease Animal Model with Microarray Analysis

초기 알츠하이머병 동물모델에서 유전자 분석 기반의 신경염증 및 뇌혈관장벽 손상 연구

2018 년 8 월

서울대학교 융합과학기술대학원
분자의학 및 바이오제약학과

서 훈 녕

Abstract

The Study of Neuroinflammation and Blood-Brain Barrier Disruption in Early Stage Alzheimer's Disease Animal Model with Microarray Analysis

Hoon Young Suh

Department of Molecular Medicine and Biopharmaceutical Science,

The Graduate School of Convergence Science and Technology,

Seoul National University

Alzheimer's disease (AD) is the most common cause of dementia, whereas little is understood about the pathogenesis of AD. Up to date, there are no effective therapy to cure or to modify the progression of AD. Since strategy for AD has shifted to prevention, researchers started to focus on the early stage of AD. To identify genetic changes in the early stage of AD, microarray analysis of the brain from 5XFAD AD model was performed. The early stage of AD was defined by Y-maze test as the time when 5XFAD mice do not show cognitive decline. At 8 months of age, 5XFAD mice significant memory deficit than normal control. 10- and 20-weeks-old 5XFAD mice were used as AD models at early stage. Immunostaining with anti-Aβ42 antibody and Thioflavin-S staining was performed to show Aβ deposit and Aβ plaque

formation, respectively. Total 55681 mRNAs were analyzed by microarray from hippocampus of 10- and 20-week-old 5XFAD mice. Furthermore, anti-Iba1 and anti-GFAP immunostaining was performed to localize the microglia and astrocyte respect to Aβ. The disruption of Blood-brain barrier (BBB) was investigated with ^{111}In-Cy3-albumin imaging. Deposition of Aβ was found in the brain of 5XFAD mice started from the age of 10 weeks, while Aβ plaque were detected at the age of 20 weeks. A total of 715 and 630 genes were differentially expressed between 5XFAD and wild type mice at 10 and 20 weeks or age, respectively (fold change > 2.0, p-value < 0.05). Genes that are associated with extracellular matrix (n = 20) and angiogenesis (n = 13) showed the significant downregulation in 10-week-old 5XFAD mice, compared to the wild type mice. Inflammation (n = 16) and immune response (n = 46) related genes were significantly upregulated in 20-week-old 5XFAD mice, compared to the wild type mice. Genes that showed continuous increase of expression from 10- to 20-week-old 5XFAD mice include Cst7, Ccl4, Ccl3, Itgax, and Clec7A. Immunostaining with anti-Iba1, anti-GFAP showed that microglial activation and astrogliosis were accompanied with Aβ in the 5XFAD mice from the age of 10 weeks. Moreover, penetration of ^{111}In-Cy3-albumin into the brain parenchyma represents the disruption of BBB. Genes that constitute BBB were downregulated in the 10-week-old 5XFAD mice, while genes that are related to inflammation and immune response were upregulated in both 10- and 20-week-old 5XFAD mice. Consequently, these results show that the neuroinflammation occurs with the disruption of BBB in the early stage of AD.

Keywords: early stage Alzheimer's disease, Alzheimer's disease animal model, neuroinflammation, blood-brain barrier, microarray

Student Number: 2016-29896

Contents

List of tables

List of figures

Introduction

Dementia is a clinical syndrome caused by neurodegenerative disorder including Alzheimer's disease (AD), vascular dementia, dementia with Lewy body, and frontotemporal dementia[1]. AD is the most common cause of dementia, accounts for 60 - 70 % of all dementia[2]. Dementia is characterized by irreversible memory impairment, cognitive decline and behavior disturbances. National Institute on Aging and the Alzheimer's Association (NIA-AA) working groups have proposed new criteria and guidelines of diagnosing preclinical, mild cognitive impairment (MCI), and established AD in 2011. Clinical diagnosis for AD is sensitive when compared to other dementias, however often reported as the specificity of 50 - 60 %[3], probably due to overlapping characteristics between other types of dementia. Much lower accuracy can be expected in the early stage of dementia when symptoms are vague[4].

Aging is one of important risk factors, as the most of AD patients present clinical symptoms at the age older than 65 years. 2 - 10 % of patients show an earlier onset of disease[5] and the minority of early-onset AD follows autosomal dominant form. Over the years, we had learned about the pathologic process of AD by the discovery of genetic factors contributing to the Mendelian form of AD: Amyloid precursor protein (APP), Presenilin 1 (PSEN1), and Presenilin 2 (PSEN2). Furthermore, Identification of at least 20 additional risky genes including the ε4 allele of Apolipoprotein E (APOE) through genome-wide association studies (GWAS) has been widened our sight[5]. The misregulation of gene transcription, translation, and protein processing are observed in AD, implying alterations in gene expression and its regulatory mechanisms[6].

Several hypotheses based on the clinical investigation of AD pathology

were suggested. Two major hypotheses are amyloid cascade hypothesis and tau hypothesis. The inflammatory hypothesis in AD has recently attracted much interest[7]. Other hypotheses for AD include: mitochondrial cascade hypothesis[8], oxidative stress hypothesis[9], vascular hypothesis[10], cholesterol hypothesis[11], metal hypothesis[12], and cell cycle hypothesis[13].

AD involves two pathological hallmarks: deposition of amyloid-ß (Aß) into amyloid plaques outside neuron and formation of tangles inside the neuron by microtubule-associated protein tau. Since deposition of Aß along with tau is the most proposed mechanism for AD, many components had been developed for the in vivo imaging of Aß and tau including ^{11}C-PiB, florbetapir (AV-45), flutemetamol (^{18}F-PiB derivative), florbetaben (AV-1), ^{18}F-T807, THK-5117, and ^{11}C-PBB3. Furthermore, a few biomarkers for AD including CSF levels of $A\beta_{42}$, total tau, and phosphorylated tau have been validated for diagnosis of AD[14]. Despite numerous studies of AD pathogenesis, still there is no effective therapeutics or inhibit the progression of clinical symptoms of AD[15].

Up to date, only four drugs: donepezil, galantamine, rivastigmine, and memantine are clinically approved, however, they have limited utility. γ-secretase is known to control the proteolysis of the transmembrane domain of the Notch receptors, and consequently, γ-secretase inhibitor on Notch receptors can control cell differentiation and gene expression. Numerous γ-secretase inhibitors have been developed for AD treatment, however, have stopped in advanced-phase clinical trials due to their severe toxic effect. Semagacestat (Eli Lilly & Co.) failed to improve clinical outcome and worsen the adverse events including skin cancers and infections[16]. Another therapeutics for AD is targeting the β-secretase or β-site APP cleaving enzyme 1 (BACE1), the first enzyme that cleaves APP. Although first- and second-generation BACE1 inhibitor failed because of their low bioavailability and toxicity, third-generation BACE1 inhibitors showed rather encouraging results in

phase II or III trials. A clinical trial with verubecestat (Merck & Co.), one of the leading BACE1 inhibitor, has been halted since it would not show positive outcome and is now in phase III trial with patients at an earlier stage[17]. Reduction of Aβ induced by monoclonal antibody (mAb) has been suggested since there was a repeated failure of clinical trials using small molecule drugs. Bapineuzumab (Pfizer, Inc., Johnson & Johnson Pharmaceutical company, Janssen Pharmaceutica and Elan Pharmaceuticals, Inc.) is a IgG1 mAb that binds $A\beta_{1-5}$. However, the phase III trial for bapineuzumab was terminated because no significant clinical benefit was seen and cerebral vasogenic edema was likely to develop in APOE4 carriers[18]. One of the mAb drugs that reached phase III trial is solaneuzumab. Solaneuzumab (Eli Lilly & Co.) is mAb that binds monomeric Aβ and targets amyloid pathology earlier in disease process[19]. Many failures of AD treatment trials may result from targeting the wrong pathological substrates. In addition, there is also a possibility that the disease status of selected patients in clinical trials are too advanced that the timing of the treatment may be too late. Appropriate therapeutic target and timing are considered as important factors that lead to the successful development of AD treatments. Since the strategy for AD has shifted to prevention[15], studies are focusing on the early stage of AD.

Besides of Aβ and tau pathology, neuroinflammation is the third possible pathological cause of AD. Microglia are the main immune cells that are activated in the injured central nervous system (CNS). In case of chronically injured brain, microglia have been shown to alter its gene expression and become sensitive to DNA damage. AD brain displayed upregulation of chemokines and chemokine receptors in response to activation of microglia-mediated neuroinflammation[20]. In addition, several small molecule drugs showed favorable results in the treatment of AD by affecting microglia inflammation. Considering that not only AD but also many neurodegenerative diseases underlie chronic insult such as aging, neuroinflammation

mediated by microglia may be involved in the early stage of neurodegenerative disease.

The main aim of this research is to investigate genetic changes in the early stage of AD using 5XFAD AD animal model. The early stage of AD was defined as time earlier than cognitive decline appears in 5XFAD mice. The early stages of AD were divided into two groups, Aβ deposit and plaque formation, by immunohistochemical staining in brain sections of 5XFAD mice. Transcriptomic study was carried out with the brain in AD, obtained from 5XFAD mice at 10 and 20 weeks of age. The results indicate that there is a notable shift in the transcriptional profile in the hippocampus of 5XFAD mice, even in the early stage of AD. In both 10- and 20-week-old 5XFAD mice, inflammation and immune response related genes showed upregulation. At 10 weeks, there was disruption of blood-brain barrier with downregulation of extracellular matrix and angiogenesis related genes. The disruption of BBB was also confirmed in 10-week-old 5XFAD mice by ^{111}In-Cy3-albumin imaging. Altogether, these data support that components that involve in BBB, inflammation, and immune response are potent mediators of the early stage of AD.

Materials and Methods

Subjects and experimental scheme

5XFAD mice which have five FAD mutations in APP and PS1 and littermates mice as wild type controls were used. The 5XFAD mouse model display AD features earlier, compared with other models[21], by developing cerebral amyloid plaques and gliosis from 2 months of age. Experimental groups were set up by behavior test with for 2, 4, 6 and 8 months of age and pathology observation for the validation of 5XFAD mice. Then, experiments including microarray, quantitative real time PCR (qPCR), immunostaining, and fluorescence imaging were performed, and the experimental scheme and the number of animals used were summarized (Supplemental Fig 1). Experiments were conducted with the approval of Institutional Animal Care and Use Committee at Seoul National University Hospital.

Y-maze test

Each mouse with different age of 2, 4, 6, and 8 months (all male, n = 7 to 14 for 5XFAD mice, n = 7 to 10 for wild type mice) was placed in the center of Y-maze and allowed to move during 8 minutes. The sequence and the total number of arms entered were measured. Percentage alternation is the product of the number of entries into three arms divided by the maximum possible alternations[22].

Immunostaining

Mice were sacrificed at 10 or 20 weeks of age after the behavioral test (n = 2 for each group). Whole brains from 5XFAD mice were harvested and fixed in phosphate-buffered 4 % paraformaldehyde at 4 ℃ for 24 hours. Fixed brains were cut into 4

um sections from coronal plane. After hydration, brain sections were incubated with citric acid buffer, 1 % H_2O_2, and blocking solution (5 % BSA and 0.5 % TritonX-100 in TBS) and stained with anti-Aß42 (BioLegend, San Diego, CA, USA; cell signaling technology, Danvers, MA, USA), anti-Iba1 (Abcam, Cambridge, UK), or anti-GFAP (Cell Signaling Technology, Danvers, MA, USA) antibodies. For Thioflavin-S staining, brain sections placed in 1 % Thioflavin S solution for 5 minutes and washed with 70 % EtOH and DW. These stained slides were captured with a LEICA confocal microscopy.

RNA extraction and quality control

Total RNA was extracted from the hippocampus in 10- or 20-week-old mice with TRIzol (Invitrogen, Carlsbad, CA, USA) reagent, according to the manufacturer's instructions. The quality of RNA was assessed by Agilent 2100 Bioanalyzer. The $OD_{260/280}$ ratio was used as an indicator for RNA purity. The 28S/18S ratio, RNA integrity number (RIN) was calculated and used for analyzing RNA integrity.

Microarray analysis

Expression profiles of all genes in total RNA from hippocampus were collected from the SurePrint G3 mouse GE 8x60K Microarray (Agilent Technologies, Waldbronn, Germany). Raw microarray signals were scanned and extracted using Agilent Feature Extraction Software. The major criteria to validate differentially expressed genes were a fold change over 2.0 or under 0.5, considering the expression values in the transgenic group relative to the wild type group. Functional classification of genes was derived from the Database for Annotation, Visualization, and Integrated Discovery (DAVID) Bioinformatics Resources 6.8 (https://david.ncifcrf.gov/)[23].

Quantification of mRNA expression

1 ug of RNA was processed into cDNA by reacting with oligo (dT) primer (Bioneer , Daejeon, Korea) and M-MLV reverse transcriptase (LeGene Biosciences , San Diego, CA, USA). For qPCR, cDNA was amplified with SYBR Premix Ex Taq (Takara, Kusatsu, Japan) on the 7500 RT-PCR system (Applied Biosystems, Carlsbad, CA, USA) and the differences in mRNA levels were calculated by the ΔΔCt method.

In vivo ^{111}In SPECT/CT imaging and ex vivo fluorescence imaging

10-week-old 5XFAD and wild type mice were intravenously injected 150 uCi/300uL ^{111}In-Cy3-albumin. After the administration, ^{111}In SPECT/CT scans were acquired on NanoSPECT/CT scanner (Bioscan, Washington, DC). All mice were anesthetized and maintained with 2.5 % isoflurane at 1 L/min oxygen flow in a prone position. SPECT images were obtained into an 80 x 80 acquisition matrix and reconstructed by a 3-dimensional ordered-subsets expectation maximum algorithm. Additional CT scans were acquired for anatomical localization. Five days after SPECT/CT acquisition, the fluorescence signals of the isolated brain were detected with IVIS Lumina Ⅱ (PerkinElmer, Waltham, MA, USA). The isolated brains were dissected and acquired fluorescence imaging in various directions. The fluorescence images were acquired using Living image software (Xenogen, Alameda, CA, USA).

Statistical analysis

The data were analyzed using SPSS Statistics 23.0 (IBM Corp., Armonk, NY, USA), Student t-test was used to compare the differences in gene expression between 5XFAD and wild type mice. To test whether the expression level was different among groups of different age and different disease status, the analysis of variance (ANOVA) was performed. A p-value < 0.05 was considered statistically significant.

Results

Behavioral changes in 8-month-old 5XFAD mice

To explore the cognitive deficits in 5XFAD mice, Y-maze test which showed spatial working memory was performed using 2-, 4-, 6-, and 8-month-old mice. 8-month-old 5XFAD mice showed a significant change in alteration, compared to the control mice (p-value < 0.05, Fig 1). Therefore, the time for 5XFAD mice to show the cognitive decline was 8 months.

Different patterns of Aß deposit between 10- and 20-week-old 5XFAD mice

To demonstrate the early stages of AD prior to cognitive deficit, the timing of Aß deposit or Aß plaque formation was determined by immunohistochemistry with Aß antibody or Thioflavin S before 8 months. 10-week-old 5XFAD mice had a small amount of Aß deposit in the cortex and hippocampus. However, the whole brain of 20-week-old 5XFAD mice was covered with Aß deposit (Fig 2). Aß plaques were presented in the brains of 20-week-old 5XFAD mice (Fig 3), while Aß plaques were not observed in the brains of 10-week-old 5XFAD mice (data not shown).

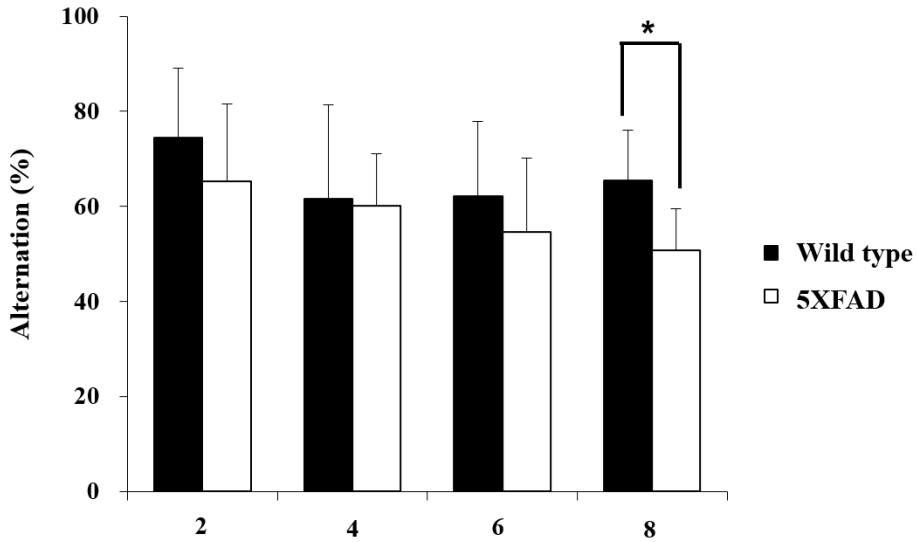

Figure 1. Y-maze test with 2-, 4-, 6-, 8-month-old 5XFAD and wild type mice

8-month-old 5XFAD mice showed a significant cognitive decline. Graphs were expressed as average ± standard deviation.

* p-value < 0.05

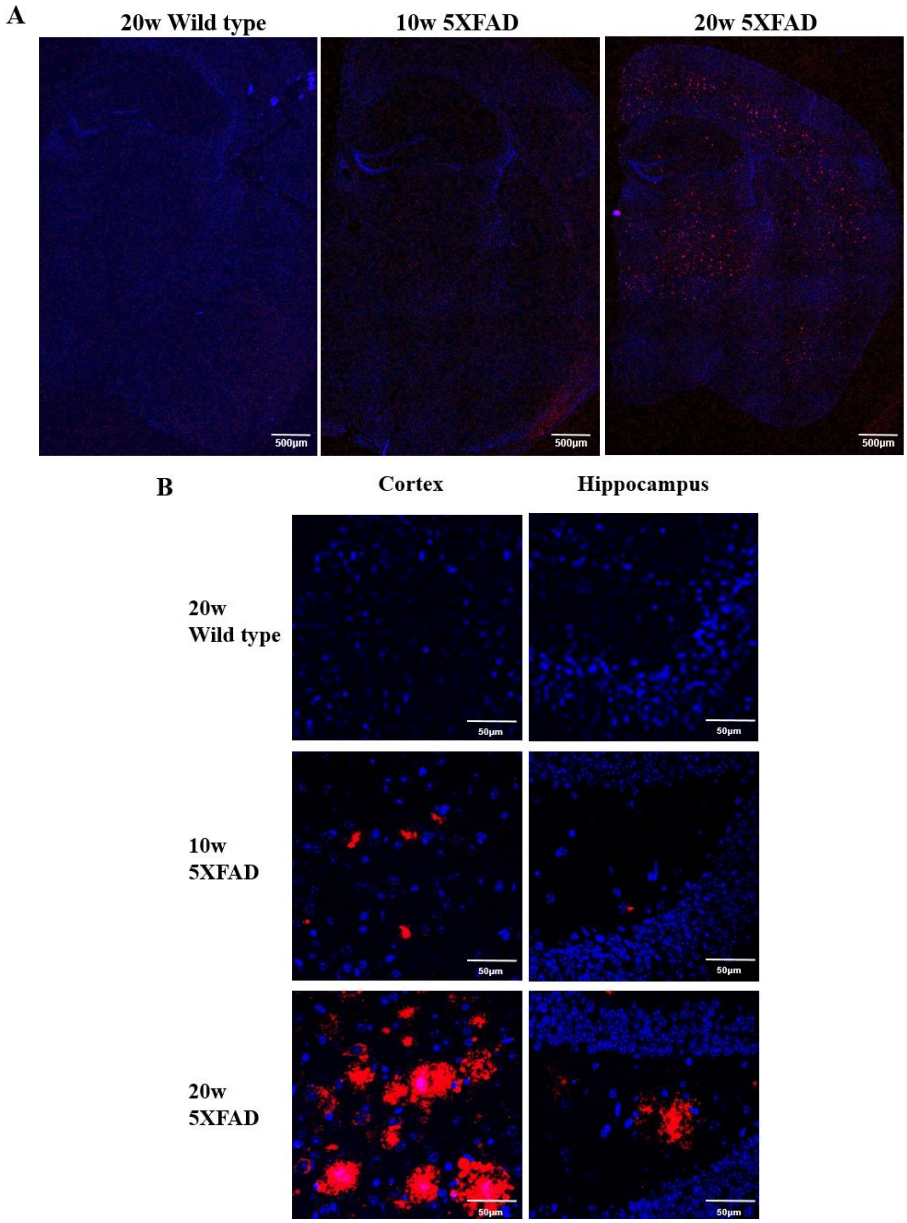

Figure 2. Anti-Aβ42 antibody staining of the brain from 10- and 20-week-old 5XFAD mice

10-week-old 5XFAD mice showed small deposition of Aß in cortex and hippocampus, while 20-week-old 5XFAD mice showed abundant deposition of Aß in the whole brain. Low (A) and high magnification images (B)

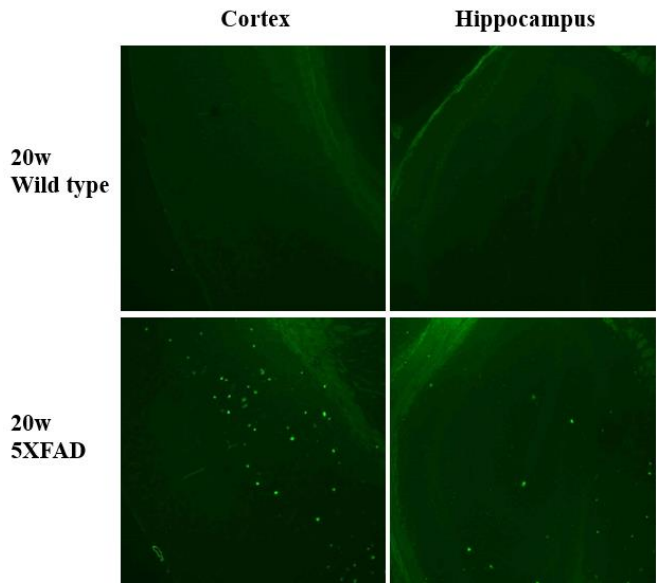

Figure 3. Thioflavin S staining of the brain from 20-week-old 5XFAD and wild type mice

20-week-old 5XFAD mice had Aß plaques in the whole brain.

Controlled quality of total RNA for microarray

The total RNA qualities from the hippocampus of 10- and 20-week-old mice were reasonable to use microarray. The $OD_{260/280}$ ratio was 2.02 ± 0.049, 28S/18S ratio and RIN were 1.11 ± 0.145 and 8.05 ± 0.3, respectively (AVE ± SD).

Distribution of gene expression in the hippocampus of 5XFAD mice

Analysis for gene ontology was performed with total 55681 mRNAs. In the microarray analysis, a total of 715 genes was differentially expressed between 10-week-old 5XFAD and wild type mice (fold change > 2.0, p-value < 0.05); 284 genes were upregulated, while 431 genes were downregulated. However, total 630 genes were differentially expressed between 20-week-old 5XFAD and wild type mice (fold change > 2.0, p-value < 0.05); 548 genes were upregulated, whereas 82 genes were downregulated (Fig 4).

Differential gene expression in the hippocampus of 5XFAD mice

In 10-week-old 5XFAD mice, most of genes had significant downregulation (fold change < 0.5, p-value < 0.05). The most prominent distinction between 10-week-old 5XFAD and wild type mice came from genes that are associated with extracellular matrix and angiogenesis (Fig 5A). The gene expression profile of 20-week-old 5XFAD and wild type mice were largely distinct from those of 10-week-old group. Upregulation of genes was dominant in 20-week-old 5XFAD mice over wild type mice. Genes known to have correlations with inflammation and immune response were upregulated in 20-week-old 5XFAD mice (fold change > 2.0, p-value < 0.05, Fig 5B).

20 and 13 downregulated genes in 10-week-old 5XFAD mice were related to extracellular matrix and angiogenesis, respectively. The genes corresponding to the upregulated mRNAs of 10-week-old 5XFAD mice included 6 genes involved in inflammation and 8 genes involved in immune response. On the contrary, the genes corresponding to the upregulated mRNAs of 20-week-old 5XFAD mice included 16 and 46 genes involving inflammation and immune response, respectively (Supplemental Table 1).

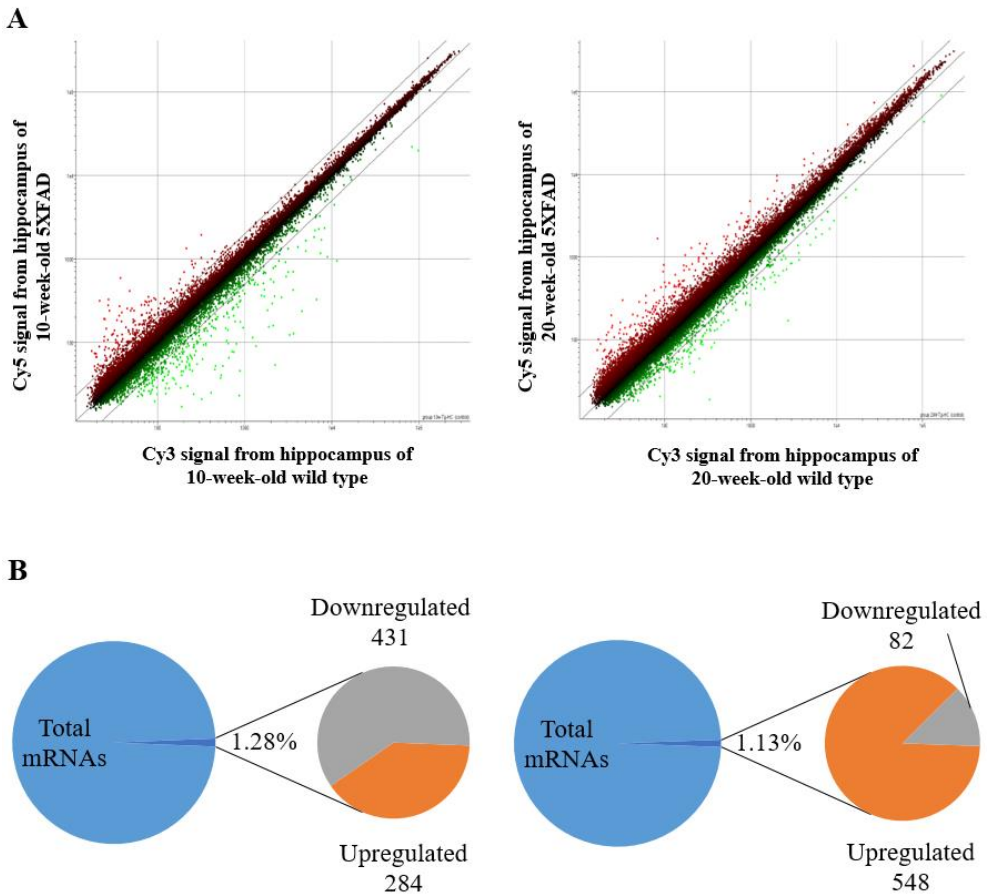

Figure 4. Distribution of total mRNAs of 10- and 20-week-old 5XFAD mice

(A) Scatter plots of the distribution of mRNAs in 10- and 20-week-old 5XFAD mice, compared with wild type. (B) 715 of 55681 (1.28%) differentially expressed mRNAs, including 284 upregulated mRNAs and 431 downregulated mRNAs in 10-week-old groups, 630 of 55681 (1.13%) differentially expressed mRNAs, including 548 upregulated and 82 downregulated mRNAs in 20-week-old groups.

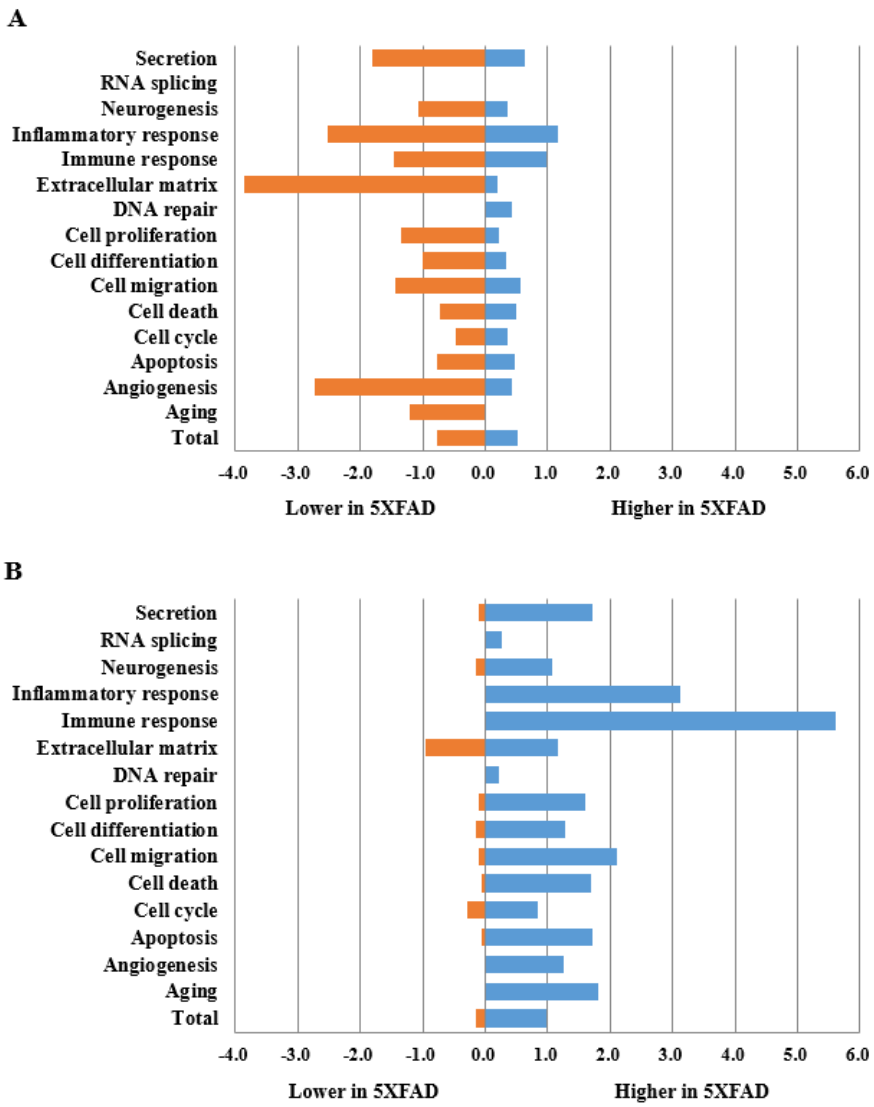

Figure 5. Gene ontology of mRNAs in 10- and 20-week-old 5XFAD mice

mRNAs that are associated with extracellular matrix and angiogenesis were significantly downregulated in 10-week-old 5XFAD mice than wild type mice. mRNAs that are related to inflammation and immune response showed significant upregulation in 10-week-old 5XFAD mice (A), even more in 20-week-old 5XFAD mice (B), compared to wild type mice.

Upregulation of genes associated with inflammation and immune system

Genes that were continuously upregulated in both 10- and 20-week-old 5XFAD mice were analyzed. The expression of Cst7 was the highest among the top five upregulated genes in 10- and 20-week-old 5XFAD mice (Table 1). The expression level of Cst7 in 20-week-old 5XFAD mice was 3-times higher than that of Cst7 in 10-week-old 5XFAD mice. Cst7 encodes cystatin F, a secreted form of type-II cysteine protease inhibitor, which is mainly expressed in immune cells[24,25]. Acting as one of enzyme regulator, Cst7 functions in protein metabolic process at extracellular region.

Other upregulated genes, Chemokine (C-C motif) ligand 4 (Ccl4), Ccl3, Integrin alpha X (Itgax), and C-type lectin domain family 7 member A (Clec7A) in 20-week-old 5XFAD mice were associated with inflammation and immune response. Both Ccl4 and Ccl3 are chemokines that enroll in receptor binding for immune process or signaling at extracellular region. Ccl4 is a strong chemoattractant of regulatory T cells[26,27]. Ccl3 helps neutrophil migrate toward the inflammatory site[28]. Itgax is a component of the plasma membrane and expressed in leukocytes including monocyte, macrophage, and neutrophil[29]. Clec7A works as a modulator in the immune process or signaling at the plasma membrane. Clec7A is expressed primarily by cells of myeloid origin, including dendritic cells[30].

To perform an independent validation of microarray data, qPCR was used (Fig 6). As same as the microarray result, upregulated genes in 10-week-old 5XFAD mice were dramatically upregulated in 20-week-old 5XFAD mice. The expression of Ccl3 was the most upregulated among the qPCR results. The early and strong upregulation of Cst7, Ccl4, Ccl3, Itgax, and Clec7A mRNA genes in the hippocampus of 5XFAD mice shows that even before cognitive decline appears,

there are translational changes for inflammation and immune response.

Downregulation of genes associated with brain homeostasis

There was a little overlap between genes of the top five downregulated genes in 10-week-old 5XFAD mice and 20-week-old 5XFAD mice. The expression level of two genes, Claudin-2 (Cldn2) and Rbbp4 were consistently low (Table 2). Claudin-2 is identified as an integral component of tight junction and expression of Cldn2 have been described to lower the transepithelial resistance[31]. Retinoblastoma-binding protein 4 (Rbbp4), also known as Rbap48, interacts with histones and modifies histone acetylation. The deficiency of Rbap48 in dentate gyrus has been suspected to be the main cause of hippocampal-dependent memory loss in normal aging[32].

Table 1. Five most upregulated genes in the hippocampus of 5XFAD mice at each age

Gene	Probe	Fold change at each age	
		10w	20w
Clcnka	A55P1976534	65.78	0.99
Cst7	A51P137419	51.42	168.40
Lrrc49	A55P2054967	45.73	0.70
Tex12	A51P116609	31.79	1.17
Olfr734	A52P457924	20.99	1.17
Ccl4	A51P509573	8.39	41.11
Ccl3	A51P140710	11.35	31.55
Itgax	A51P303424	7.04	21.88
Clec7a	A51P246653	6.92	20.15

Fold changes compared to hippocampus from wild type mice are indicated in red when > 2.0

A

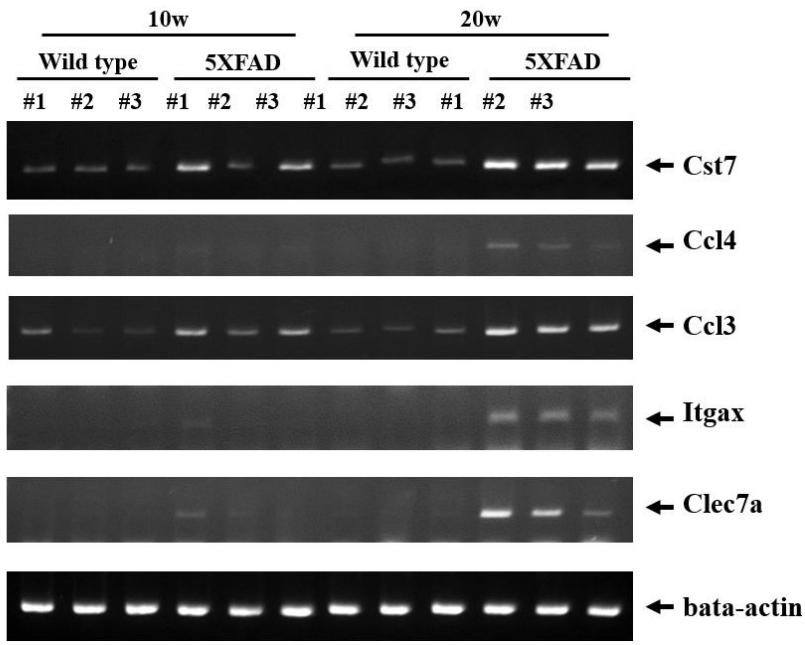
10w
20w
Wild type
5XFAD
Wild type
5XFAD
#1 #2 #3 #1 #2 #3 #1 #2 #3 #1 #2 #3
Cst7
Ccl4
Ccl3
Itgax
Clec7a
bata-actin

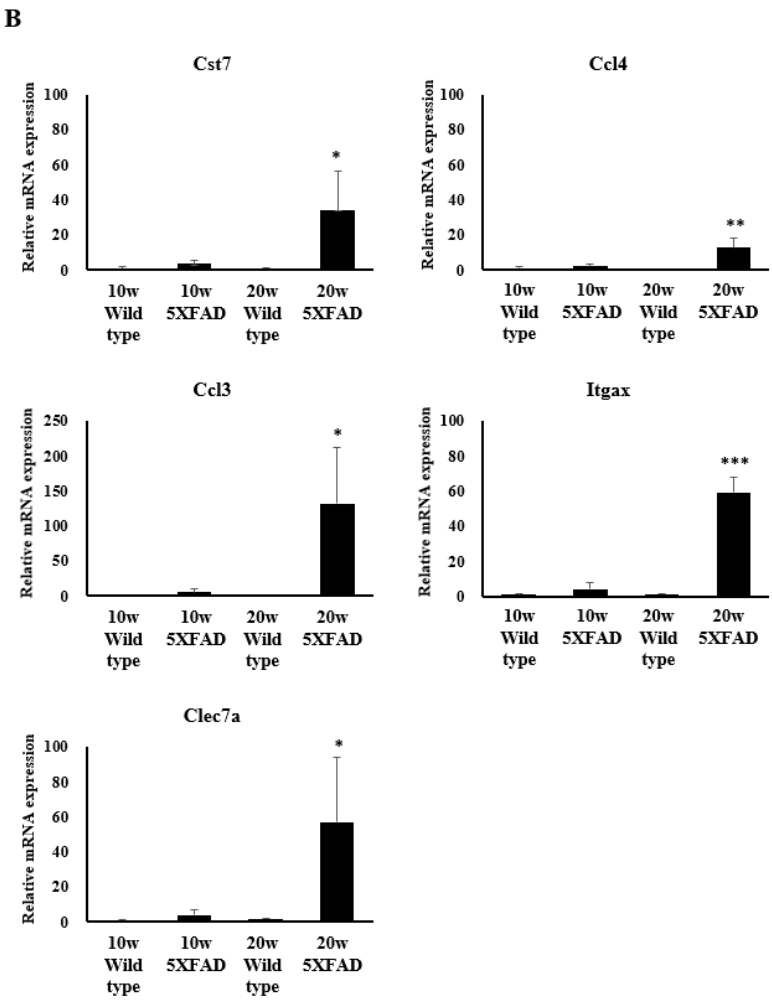

Figure 6. PCR analyses of five most upregulated genes in the hippocampus of 5XFAD and wild type mice

The result of PCR analysis (A). The average levels of Cst7, Ccl3, Itgax, and Clec7a of 20-week-old 5XFAD mice were 10-fold higher than 10-week-old 5XFAD mice in the qPCR analysis (B). Beta-actin was measured in the same samples as positive control. Graphs depict the average ± standard deviation of results.

* p-value < 0.05, ** p-value < 0.01, *** p-value <0.005

Table 2. Five most downregulated genes in the hippocampus of 5XFAD mice at each age

Gene	Probe	Fold change at each age	
		10w	20w
Ap4s1	A66P105711	0.01	0.99
LOC100041550	A55P1998110	0.01	0.81
Vmn1r167	A55P2077479	0.01	1.31
Gm3081	A55P1958324	0.01	1.23
Fbxw22	A52P1194572	0.02	1.17
Mmp1a	A55P1984546	1.14	0.04
Magea10	A55P2131213	1.14	0.06
Cldn2	A52P251450	0.07	0.10
Gm3750	A55P1959849	1.14	0.10
Rbbp4	A52P424767	0.13	0.10

Fold changes compared to hippocampus from wild type mice are indicated in red when < 0.5.

Association of immune cells with Aß deposit

To confirm that the inflammation and immune responses in the microarray analysis were increased, brain sections of 10- and 20-week-old 5XFAD mice were stained using anti-Aβ42 antibody with microglial marker Iba1, or astrocyte marker GFAP antibody. Activation of microglia (Fig 7) and astrogliosis (Fig 8) were accompanied with Aβ deposit in the brain of 5XFAD mice from 10 weeks of age. At 20 weeks of age, the Aβ deposit was much more surrounded by microglia and astrocyte in the cortex, dentate gyrus, and cornu ammonis of 5XFAD mice than 10 weeks of age.

Disruption of blood-brain barrier in the early stage of AD

Microarray analysis showed that Ccl4, Ccl3, Itgax, and Clec7A among the upregulated genes induce migration of regulatory T cells or neutrophils, or increased leukocytes including monocytes, macrophages, and neutrophils. This indicates the infiltration of myeloid cells through the disruption of BBB. Therefore, ^{111}In- and cy3- double-labeled albumin were administered intravenously in order to confirm the disruption of BBB in 10-week-old 5XFAD mice. ^{111}In of albumin was observed by SPECT/CT, however, there was no significant difference of distribution of albumin between 5XFAD and wild type mice at 10 weeks of age (Data not shown). Five days after SPECT acquirement, albumin fluorescence was observed through IVIS, and fluorescence signals were observed in the cortex, pons, medulla, and cerebellum of 5XFAD mice (Fig 9). 18-month-old 5XFAD mice as a positive control showed strong albumin signals, and these results implied that the disruption of BBB began to occur at 10 weeks of age.

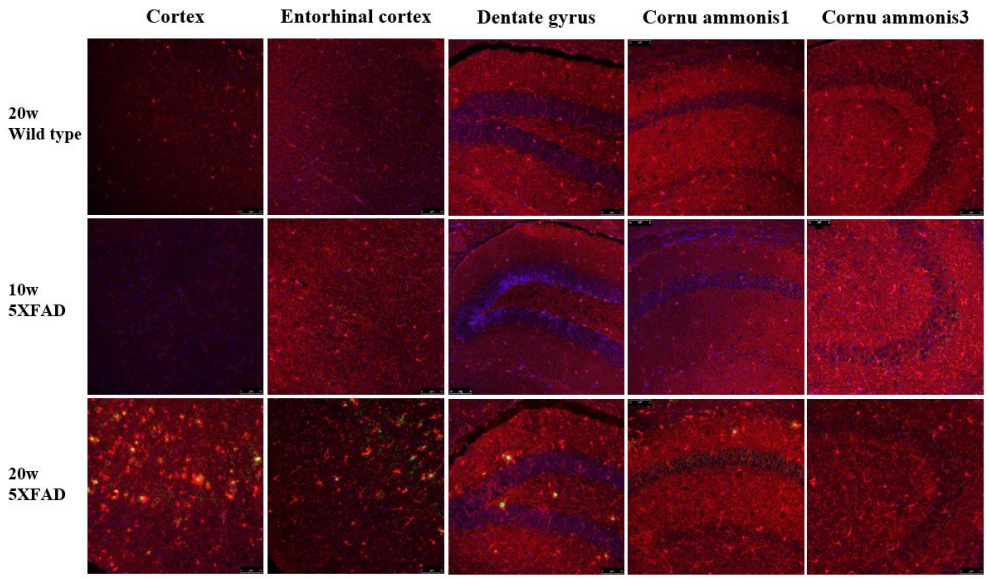

Figure 7. Immunolocalization of Aβ and microglia

Aβ deposit localize near activated microglia in the cortex, dentate gyrus, and cornu ammonis in 20-week-old 5XFAD mice. Mixed cultures from mouse brain stained with antibody to Iba1(red), Aβ (green), and DAPI (blue).

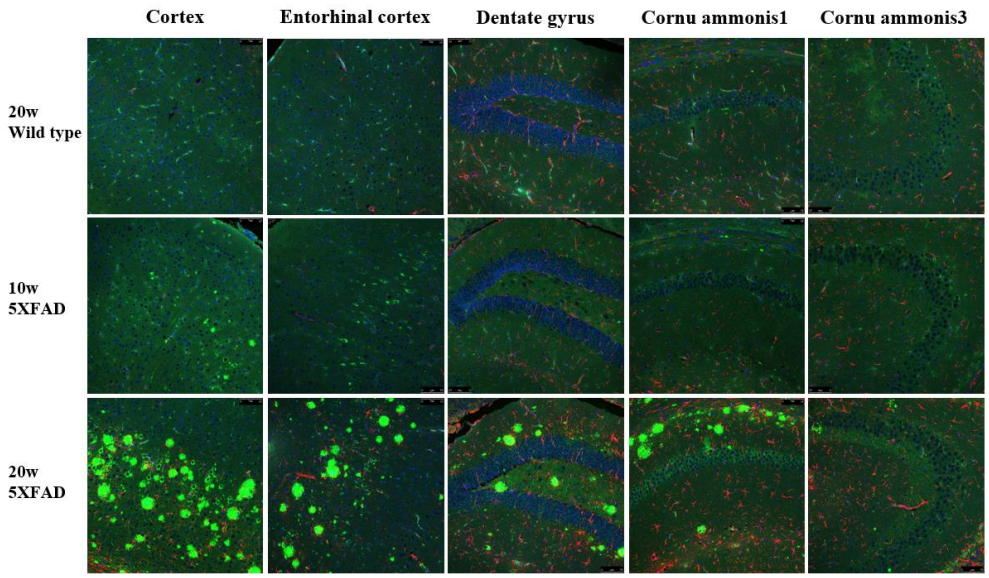

Figure 8. Immunolocalization of Aβ and astrocyte

Astrocytes are more prominent along Aβ deposit in the cortex, dentate gyrus, and cornu ammonis1 in 20-week-old 5XFAD mice. Mixed cultures from mouse brain stained with antibody to GFAP(red), Aβ (green), and DAPI (blue).

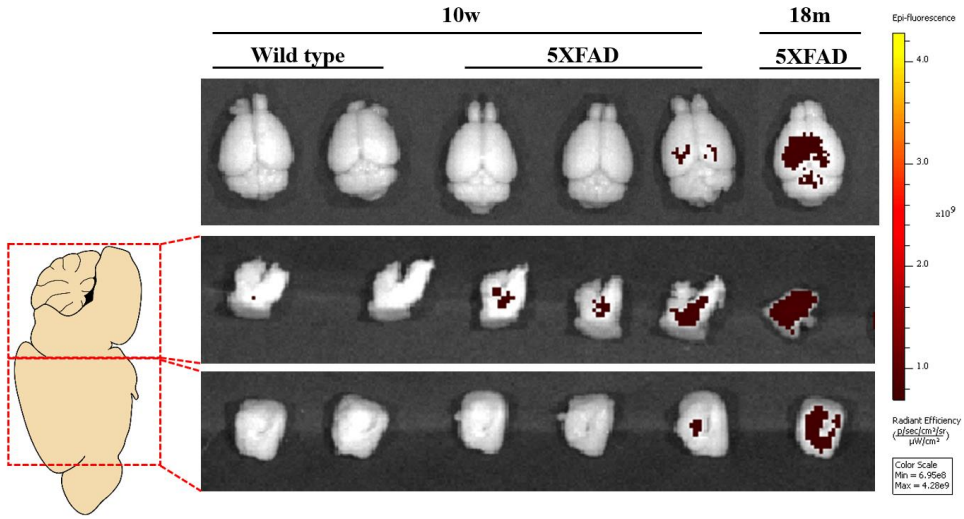

Figure 9. Distribution of albumin double labeled by ^{111}In and fluorescence

Albumin was present in the brain of 10-week-old 5XFAD mice through disrupted BBB, which was confirmed by ex vivo fluorescence imaging. An 18-month-old 5XFAD mouse was used as positive control.

Discussion

In this study, deposition of Aß in the brain of 5XFAD mice was started as early as 10 weeks of age and the Aß plaques in the brain of 5XFAD mice at 20 weeks of age. These results are consistent with the previous findings that Aß deposit in hippocampus and cortex begins at 2 months of age and spreads by 6 months of age in 5XFAD mice[21]. Concomitant with the onset of Aß deposit and plaque formation, 5XFAD mice exhibit impairments in hippocampus-dependent memory at 8 months of age.

Intravenously administered albumin was presented in the brain of 10-week-old 5XFAD mice and this suggests the movement of albumin across the BBB (Fig 9). BBB functions as a protective barrier that shields the CNS from circulating agents and is composed at the level of cerebral capillary endothelial cells through tight junction formation. The tight junction present between the cerebral endothelial cells and work as a selective barrier for blood-borne substances[33]. Cldn2, which encodes for tight junction protein Claudin-2, was downregulated in the early stage of AD. Since upregulation of Cldn2 causes transformation of 'tight' tight junction to leaky one[31], there is a possibility to activate protective mechanism from the disruption of BBB by suppressing the expression of Cldn2, consequently, strengthening the tight junction. On the other hand, downregulation of tight junction protein can cause bulk flow transcytosis across the BBB, causing disruption of BBB[34].

Another component of BBB is basement membrane that encloses cerebral endothelial cells and pericytes and forms perivascular extracellular matrix[35]. Downregulation of genes that are associated with extracellular matrix and angiogenesis was shown in 10-week-old 5XFAD mice. The decrease of components that consist extracellular matrix of BBB may loosen the BBB. The decrease of

angiogenesis may result in dysregulation of cerebral endothelial cells and the disruption of BBB. Based on the two-hit vascular hypothesis of AD, cerebrovascular dysfunction leads to a decrease in brain perfusion, therefore, causes neuronal loss and Aß deposit in AD[36].

The previously dominant hypothesis for AD pathogenesis is that Aß plaques could result in inflammation in the brain through activation of glial cells[37]. Even regarded as an immune-privileged site, CNS is set for innate immune responses, mainly by microglia and astrocytes. Microglia plays the role of a cerebral macrophage and recruits reactive A1 astrocyte. Secretion of Il-1α, TNF, and C1q from microglia have reported inducing activation of astrocyte[38]. The astrocyte is the most abundant glial cell and releases mediators to maintain brain homeostasis[39]. Reactive astrocytes exist at least two different types of activation, A1 and A2, and neurotoxic A1 reactive astrocytes are present in neurodegenerative brain regions[38]. Presence of A1 reactive astrocyte in Alzheimer's disease suggests that neuroinflammation might help or drive neurodegeneration[40]. This also correlates with our data that inflammation and immune response in transcriptional level precede the deposition of Aß. Microarray analysis revealed that the number of differentially expressed genes increased with age in the hippocampus of the 5XFAD mice. In the 20-week-old group, twice as many genes are upregulated more than two-fold in the hippocampus, compared to the 10-week-old group. Therefore, this result suggests that transcriptional shift starts from the early stage of AD.

Genes associated with the inflammatory and immunological process were upregulated in 20-week-old 5XFAD mice three times more than 10-week-old 5XFAD mice. In other words, upregulated genes at early stage of AD were related to the inflammatory and immunological process. What exact mechanism underlies remains controversy, however, one possible route is through microglial activation. A recent study analyzed AD mouse model and showed that some microglia change

their gene expression profile as the disease progresses. The disease-induced transition of gene expression in microglia was called as disease associated microglia (DAM) profile[41]. Among upregulated genes in the hippocampus of both 10- and 20-week-old 5XFAD mice, Cst7, Itgax, and Clec7A were correlated with DAM profile of 8-month-old 5XFAD mice. Thus, these findings lead to the suggestion that the microglia activate through transcriptional modification even much earlier than the previous studies, and eventually cause neuroinflammation.

Increased expression of chemokines, Ccl4 and Ccl3, may suggest activation of the adaptive immune system in the early stage of AD. Several studies had attributed that microglia could be sensitive to the chemokines[42,43], therefore exacerbates Aβ deposit and neuronal loss[44]. Not only glial cells but also neurons express chemokines including Ccl3 under degenerative condition[45]. Migration of peripheral immune cells including T cells, monocyte, and neutrophils through compromised BBB could contribute to neuroinflammation in AD[46]. During neurodegeneration in AD, most of the migrating cells from cerebral blood vessel to parenchyma via BBB were neutrophils in 5XFAD mice[47]. Ccl4 and Ccl3 also induce syntheses of pro-inflammatory molecules, such as IL-1 or IL-6[48], thereby propagate neuroinflammation.

Although microarray analysis can survey a large group of genes, microarray analysis has limitations such as quantitation, errors due to background noise, and false positive results. Therefore, further experiments are needed to verify the expression level of the specific genes found by microarray analysis. Another consideration is that protein is a key mediator to regulate physiological condition, so it needs to verify whether the changes in gene expression are directly indicative of the physiological process. To understand the etiology and pathology of the early stage of AD, specific genes from microarray analysis should estimate the changes in protein expression or functional evaluation in AD. In this study, although a small

number of samples were used, the experimental results can be relied upon to verify similar expression changes in the same animal model (Fig 6).

Conclusion

The question addressed by this study is what kind of genetic change is occurred in the early stage of AD, prior to the cognitive decline. 10-week-old 5XFAD mice showed the transition of albumin through disrupted BBB and downregulation of genes that constitute BBB. 20-week-old 5XFAD mice had upregulation of inflammation and immune response related genes. Altogether, this study gives supporting evidence that neuroinflammation accompanied by leaky BBB constitute a pathogenic pathway in the early stage of AD.

References

1. Prince M, Bryce R, Albanese E, Wimo A, Ribeiro W, Ferri CP. The global prevalence of dementia: A systematic review and metaanalysis. *Alzheimer's & Dementia*. 2013;9(1):63-75.e62.
2. Wilson RS, Segawa E, Boyle PA, Anagnos SE, Hizel LP, Bennett DA. The natural history of cognitive decline in Alzheimer's disease. *Psychology and Aging*. 2012;27(4):1008-1017.
3. Mayeux R, Saunders AM, Shea S, et al. Utility of the Apolipoprotein E genotype in the diagnosis of Alzheimer's disease. *New England Journal of Medicine*. 1998;338(8):506-511.
4. Paolacci L, Giannandrea D, Mecocci P, Parnetti L. Biomarkers for early diagnosis of Alzheimer's disease in the oldest old: Yes or No? *Journal of Alzheimer's Disease*. 2017;58(2):323-335.
5. Van Cauwenberghe C, Van Broeckhoven C, Sleegers K. The genetic landscape of Alzheimer disease: clinical implications and perspectives. *Genetics in Medicine*. 2015;18:421.
6. Selkoe DJ. Alzheimer's disease: genes, proteins, and therapy. *Physiological Reviews*. 2001;81(2):741-766.
7. Zotova E, Nicoll JAR, Kalaria R, Holmes C, Boche D. Inflammation in Alzheimer's disease: relevance to pathogenesis and therapy. *Alzheimer's Research & Therapy*. 2010;2(1):1.
8. Swerdlow RH, Burns JM, Khan SM. The Alzheimer's disease mitochondrial cascade hypothesis. *Journal of Alzheimer's Disease*. 2010;20(Suppl 2):265-279.
9. Markesbery WR. Oxidative stress hypothesis in Alzheimer's disease. *Free*

Radical Biology and Medicine. 1997;23(1):134-147.

10. de la Torre JC. The vascular hypothesis of Alzheimer's disease: bench to bedside and beyond. *Neurodegenerative Diseases.* 2010;7(1-3):116-121.
11. Wood WG, Li L, Müller WE, Eckert GP. Cholesterol as a causative factor in Alzheimer's disease: a debatable hypothesis. *Journal of Neurochemistry.* 2014;129(4):559-572.
12. Bush AI, Tanzi RE. Therapeutics for Alzheimer's disease based on the metal hypothesis. *Neurotherapeutics.* 2008;5(3):421-432.
13. Neve RL, McPhie DL. The cell cycle as a therapeutic target for Alzheimer's disease. *Pharmacology & Therapeutics.* 2006;111(1):99-113.
14. Wang J, Gu BJ, Masters CL, Wang Y-J. A systemic view of Alzheimer disease — insights from amyloid-β metabolism beyond the brain. *Nature Reviews Neurology.* 2017;13:612.
15. Graham WV, Bonito-Oliva A, Sakmar TP. Update on Alzheimer's disease therapy and prevention strategies. *Annual Review of Medicine.* 2017;68(1):413-430.
16. Doody RS, Raman R, Farlow M, et al. A Phase 3 Trial of semagacestat for treatment of Alzheimer's disease. *New England Journal of Medicine.* 2013;369(4):341-350.
17. Hawkes N. Merck ends trial of potential Alzheimer's drug verubecestat. *British Medical Journal.* 2017;356.
18. Vandenberghe R, Rinne JO, Boada M, et al. Bapineuzumab for mild to moderate Alzheimer's disease in two global, randomized, phase 3 trials. *Alzheimer's Research & Therapy.* 2016;8(1):18.
19. Siemers ER, Sundell KL, Carlson C, et al. Phase 3 solanezumab trials: secondary outcomes in mild Alzheimer's disease patients. *Alzheimer's & Dementia.* 2016;12(2):110-120.

20. Ransohoff RM. Chemokines and chemokine receptors: standing at the crossroads of immunobiology and neurobiology. *Immunity.* 2009;31(5):711-721.

21. Oakley H, Cole SL, Logan S, et al. Intraneuronal β-Amyloid aggregates, neurodegeneration, and neuron loss in transgenic mice with five familial Alzheimer's disease mutations: potential factors in amyloid plaque formation. *The Journal of Neuroscience.* 2006;26(40):10129-10140.

22. Ohno M, Cole SL, Yasvoina M, et al. BACE1 gene deletion prevents neuron loss and memory deficits in 5XFAD APP/PS1 transgenic mice. *Neurobiology of Disease.* 2007;26(1):134-145.

23. Dennis G, Sherman BT, Hosack DA, et al. DAVID: Database for annotation, visualization, and integrated discovery. *Genome Biology.* 2003;4(9):R60.

24. Morita M, Hara Y, Tamai Y, Arakawa H, Nishimura S. Genomic construct and mapping of the gene for CMAP (Leukocystatin/Cystatin F, CST7) and identification of a proximal novel gene, BSCv (C20orf3). *Genomics.* 2000;67(1):87-91.

25. Ni J, Fernandez MA, Danielsson L, et al. Cystatin F is a glycosylated human low molecular weight cysteine proteinase inhibitor. *The Journal of Biological Chemistry.* 1998;273(38):24797-24804.

26. Bystry RS, Aluvihare V, Welch KA, Kallikourdis M, Betz AG. B cells and professional APCs recruit regulatory T cells via CCL4. *Nature Immunology.* 2001;2(12):1126-1132.

27. Xia MQ, Hyman BT. Chemokines/chemokine receptors in the central nervous system and Alzheimer's disease. *Journal of Neurovirology.* 1999;5(1):32-41.

28. Ramos CD, Canetti C, Souto JT, et al. MIP-1alpha[CCL3] acting on the CCR1 receptor mediates neutrophil migration in immune inflammation via

sequential release of TNF-alpha and LTB4. *Journal of Leukocyte Biology.* 2005;78(1):167-177.

29. Takada Y, Ye X, Simon S. The integrins. *Genome Biology.* 2007;8(5):215.
30. Taylor PR, Brown GD, Reid DM, et al. The beta-glucan receptor, dectin-1, is predominantly expressed on the surface of cells of the monocyte/macrophage and neutrophil lineages. *Journal of Immunology.* 2002;169(7):3876-3882.
31. Amasheh S, Meiri N, Gitter AH, et al. Claudin-2 expression induces cation-selective channels in tight junctions of epithelial cells. *Journal of Cell Science.* 2002;115(24):4969-4976.
32. Pavlopoulos E, Jones S, Kosmidis S, et al. Molecular mechanism for age-related memory loss: the histone-binding protein RbAp48. *Science Translational Medicine.* 2013;5(200):200ra115-200ra115.
33. Ballabh P, Braun A, Nedergaard M. The blood–brain barrier: an overview: structure, regulation, and clinical implications. *Neurobiology of Disease.* 2004;16(1):1-13.
34. Armulik A, Genové G, Mäe M, et al. Pericytes regulate the blood–brain barrier. *Nature.* 2010;468:557.
35. Abbott NJ, Patabendige AAK, Dolman DEM, Yusof SR, Begley DJ. Structure and function of the blood–brain barrier. *Neurobiology of Disease.* 2010;37(1):13-25.
36. Zlokovic BV. Neurovascular pathways to neurodegeneration in Alzheimer's disease and other disorders. *Nature Reviews Neuroscience.* 2011;12:723.
37. Heneka MT, Carson MJ, Khoury JE, et al. Neuroinflammation in Alzheimer's disease. *The Lancet Neurology.* 2015;14(4):388-405.
38. Liddelow SA, Guttenplan KA, Clarke LE, et al. Neurotoxic reactive astrocytes are induced by activated microglia. *Nature.* 2017;541:481.

39. Farina C, Aloisi F, Meinl E. Astrocytes are active players in cerebral innate immunity. *Trends in Immunology.* 2007;28(3):138-145.

40. Liddelow SA, Barres BA. Reactive astrocytes: production, function, and therapeutic potential. *Immunity.* 2017;46(6):957-967.

41. Keren-Shaul H, Spinrad A, Weiner A, et al. A unique microglia type associated with restricting development of Alzheimer's disease. *Cell.* 2017;169(7):1276-1290. e1217.

42. Flynn G, Maru S, Loughlin J, Romero IA, Male D. Regulation of chemokine receptor expression in human microglia and astrocytes. *Journal of Neuroimmunology.* 2003;136(1):84-93.

43. Ubogu EE, Cossoy MB, Ransohoff RM. The expression and function of chemokines involved in CNS inflammation. *Trends in Pharmacological Sciences.* 2006;27(1):48-55.

44. Piirainen S, Youssef A, Song C, et al. Psychosocial stress on neuroinflammation and cognitive dysfunctions in Alzheimer's disease: the emerging role for microglia? *Neuroscience & Biobehavioral Reviews.* 2017;77:148-164.

45. Biber K, Zuurman MW, Dijkstra IM, Boddeke HWGM. Chemokines in the brain: neuroimmunology and beyond. *Current Opinion in Pharmacology.* 2002;2(1):63-68.

46. Le Page A, Dupuis G, Frost EH, et al. Role of the peripheral innate immune system in the development of Alzheimer's disease. *Experimental Gerontology.* 2018;107:59-66.

47. Zenaro E, Pietronigro E, Bianca VD, et al. Neutrophils promote Alzheimer's disease–like pathology and cognitive decline via LFA-1 integrin. *Nature Medicine.* 2015;21:880.

48. Bagyinszky E, Giau VV, Shim K, Suk K, An SSA, Kim S. Role of

inflammatory molecules in the Alzheimer's disease progression and diagnosis. *Journal of the Neurological Sciences.* 2017;376:242-254.

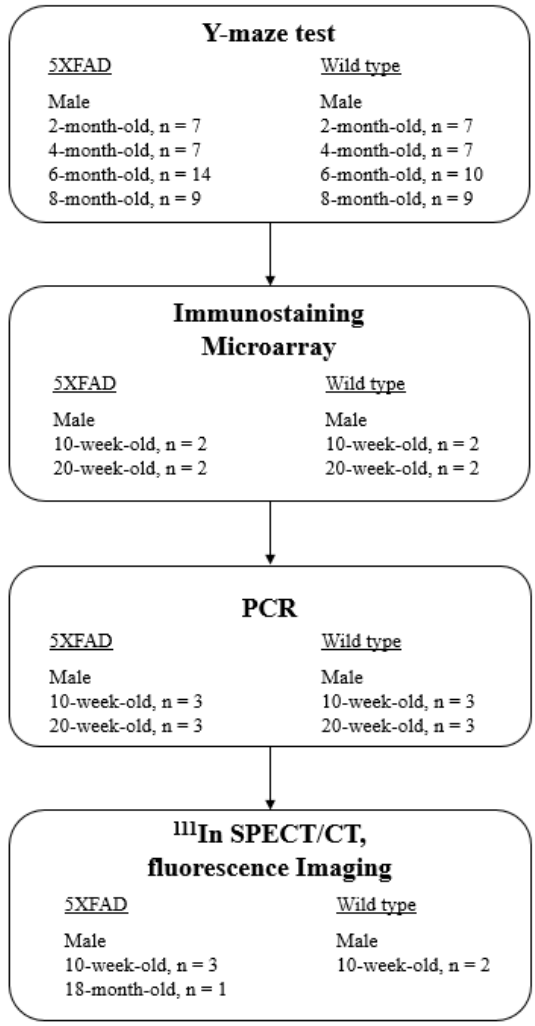

Supplemental Figure 1. Scheme of animal experiments

Supplemental Table 1. Downregulated or upregulated genes in 5XFAD mice

Ontology	Gene	Probe	P-value	Fold change
10w 5XFAD vs. 10w Wild type				
Extracellular matrix	Adamts19	A51P103054	0.00	0.09
	Col8a1	A52P292792	0.16	0.12
	Col8a2	A52P302544	0.14	0.16
	Gpld1	A55P2054673	0.01	0.19
	Col9a3	A66P101732	0.06	0.23
	Omd	A51P342926	0.02	0.25
	Col8a2	A55P1960631	0.10	0.26
	Frem1	A55P1999641	0.07	0.28
	Col15a1	A55P2060386	0.10	0.30
	Sfrp1	A66P134428	0.08	0.31
	Pcolce	A55P2020577	0.19	0.32
	Fmod	A51P207622	0.02	0.35
	Col18a1	A55P2124791	0.20	0.35
	Nid2	A51P315666	0.14	0.40
	Mgp	A51P426270	0.02	0.42
	Fbln5	A55P2088615	0.03	0.46
	Col14a1	A55P2124736	0.16	0.47
	Mfap5	A55P2062777	0.31	0.48
	Crispld2	A55P2052016	0.23	0.49
	Sod3	A55P2077558	0.03	0.50
Angiogenesis	Aqp1	A51P125205	0.11	0.04
	Col8a1	A52P292792	0.16	0.12
	Sulf1	A55P1957424	0.21	0.16
	Col8a2	A52P302544	0.14	0.16
	Sulf1	A51P142744	0.17	0.16
	Lepr	A55P2192662	0.14	0.17
	Gpld1	A55P2054673	0.01	0.19
	Col8a2	A55P1960631	0.10	0.26
	Cd59a	A51P142896	0.06	0.32
	Col18a1	A55P2124791	0.20	0.35

	Sphk1	A55P2186005	0.04	0.41
	Lepr	A55P2177911	0.09	0.45
	Crhr2	A55P1987156	0.14	0.46
Inflammation	Ccl3	A51P140710	0.02	11.35
	Agtr2	A51P437978	0.03	2.70
	Nlrp3	A55P2273439	0.04	2.34
	Tlr12	A66P114333	0.01	2.13
	Nod2	A55P2359797	0.04	2.12
	Ly86	A51P465350	0.02	2.07
Immune response	Ccl3	A51P140710	0.02	11.35
	Lat2	A51P242930	0.00	3.41
	Apoa4	A51P327491	0.03	2.84
	Tbx21	A51P501364	0.02	2.32
	Tlr12	A66P114333	0.01	2.13
	Nod2	A55P2359797	0.04	2.12
	Ly86	A51P465350	0.02	2.07
	Thy1	A55P2072035	0.01	2.04
20w 5XFAD vs. 20w Wild type				
Immune response	Ccl4	A51P509573	0.00	41.11
	Ccl3	A51P140710	0.03	31.55
	Clec7a	A51P246653	0.00	20.15
	Ccl6	A51P460954	0.02	6.25
	Dhx58	A52P223809	0.00	5.78
	Oas1a	A55P1998942	0.00	5.72
	Tyrobp	A51P261517	0.00	4.78
	Oas1a	A55P1998943	0.00	4.61
	Bcl3	A55P2066116	0.03	3.95
	Card11	A51P316042	0.00	3.83
	Tnfsf8	A55P2179463	0.01	3.80
	Bcl2a1d	A55P1978424	0.00	3.68
	C4b	A55P2078633	0.01	3.58
	Slc11a1	A51P186476	0.00	3.50
	Endou	A55P2066559	0.00	3.41

	Ly86	A51P465350	0.01	3.30
	Lag3	A51P264825	0.00	3.26
	Tbx21	A51P501364	0.01	3.02
	Il2ra	A55P1980796	0.04	2.87
	Myo1f	A66P112305	0.00	2.77
	Fcer1g	A51P405476	0.02	2.71
	Ciita	A55P2179074	0.02	2.70
	Myo1f	A55P2124273	0.00	2.70
	Prg4	A55P2185860	0.05	2.70
	Thy1	A55P2072035	0.01	2.61
	Mx1	A55P2118441	0.04	2.60
	Ccl9	A51P185660	0.00	2.60
	Sp110	A55P2152566	0.01	2.54
	Cd79b	A51P342652	0.02	2.53
	C3ar1	A51P282557	0.04	2.51
	Irf8	A52P354823	0.01	2.47
	Sbno2	A55P1959496	0.01	2.44
	Cd86	A55P1971951	0.05	2.43
	Il1rl1	A55P2027737	0.04	2.41
	Tnfaip8l2	A51P150678	0.02	2.33
	Fgr	A52P456640	0.04	2.28
	Vav1	A55P2036567	0.01	2.23
	C1rb	A52P114260	0.02	2.22
	C4bp	A52P60194	0.01	2.15
	Map3k14	A55P1988664	0.00	2.15
	Cd37	A55P2174490	0.01	2.11
	Cyba	A55P1979341	0.01	2.03
	Zbp1	A55P1994042	0.02	2.02
	Fes	A52P635338	0.01	2.01
	Gbp6	A55P2052380	0.01	2.00
	Jak3	A55P2010912	0.01	2.00
Inflammation	Ccl4	A51P509573	0.00	41.11
	Ccl3	A51P140710	0.03	31.55

Clec7a	A51P246653	0.00	20.15
C4b	A55P2078633	0.01	3.58
Slc11a1	A51P186476	0.00	3.50
Naip2	A55P1984243	0.00	3.47
Ly86	A51P465350	0.01	3.30
Serpinf2	A55P1956497	0.00	3.14
Il2ra	A55P1980796	0.04	2.87
Fcer1g	A51P405476	0.02	2.71
Sbno2	A55P1959496	0.01	2.44
Il1rl1	A55P2027737	0.04	2.41
Tnfaip8l2	A51P150678	0.02	2.33
Pik3cg	A55P2126033	0.02	2.24
Pik3cg	A51P507832	0.01	2.22
Cyba	A55P1979341	0.01	2.03

국 문 초 록

초기 알츠하이머병 동물모델에서 유전자 분석 기반의 신경염증 및 뇌혈관장벽 손상 연구

서훈녕

서울대학교

융합과학기술대학원

분자의학 및 바이오제약학과

알츠하이머병은 치매 중 가장 흔한 질환으로 병인론에 대해서는 일부만이 밝혀져있다. 알츠하이머병의 완치제나 병의 진행을 늦추는 치료제는 아직 없다. 따라서 알츠하이머병에 대한 치료 전략은 예방에 초점이 맞춰지고 있으며, 그로 인해 초기 알츠하이머병에 대한 관심이 증가하고 있다. 초기 알츠하이머병의 유전자 변화를 알아보기 위해서 알츠하이머병 동물모델인 5XFAD의 뇌를 얻어 마이크로어레이(microarray)를 시행하였다. 초기 알츠하이머병은 Y 미로 실험에서 인지 장애를 보이는 시점을 기준으로 정의하였다. 8개월령 5XFAD에서 정상 쥐에 비해 유의한 기억력 저하를 보였고, 초기 알츠하이머병에 대한 분석을 위해 10주령, 20주령 5XFAD이 사용되었다. 항 아밀로이드 베타(Aβ)42 항체를 사용한 면역 염색과 Thioflavin-S 염색으로 각각 Aβ

침착과 아밀로이드반의 형성을 확인하였다. Microarray로 10주령, 20주령 5XFAD의 해마를 사용하여 총 55681개의 mRNA를 분석하였다. 항 Iba1, 항 GFAP 면역염색으로 Aβ 침착 주변의 미세아교세포, 성상세포의 위치를 확인하였다. 뇌혈관장벽의 손상은 ^{111}In−Cy3−알부민 영상으로 관찰하였다. Aβ 침착은 10주령부터 관찰되었고, 아밀로이드반의 형성은 20주령에서 확인이 되었다. 10주령과 20주령 5XFAD에서 총 715개, 630개의 유전자가 대조군과 다른 발현을 보였다(fold change > 2, p-value < 0.05). 10주령 5XFAD에서 세포외기질 (n = 20), 혈관신생 (n = 13)과 관련된 유전자들의 발현이 대조군에 비해 감소하였고, 20주령 5XFAD에서 염증 (n = 16), 면역 반응 (n = 46)과 관련된 유전자들의 발현이 대조군에 비해 증가하였다. 10주부터 20주까지 5XFAD에서 지속적으로 발현이 증가된 유전자들은 Cst7, Ccl4, Ccl3, Itgax, Clec7A였다. 항 Iba1, 항 GFAP 면역염색에서 미세아교세포와 성상세포의 활성화가 10주령 5XFAD에서 Aβ 침착 주변에서 관찰되었다. 또한 뇌에서의 ^{111}In−Cy3−알부민이 관찰되었고 이는 뇌혈관장벽의 손상을 의미한다. 본 연구에서 10주령 5XFAD에서 뇌혈관장벽을 구성하는 유전자의 발현이 감소되었고, 10주령과 20주령 5XFAD에서 염증, 면역 반응과 관련된 유전자의 발현이 증가하였다. 이는 초기 알츠하이머병에서 뇌혈관장벽의 손상과 함께 신경염증이 일어남을 보여준다.

주요어: 초기 알츠하이머병, 알츠하이머병 동물모델, 신경염증, 뇌혈관장벽, 유전자 분석

학번: 2016-29896